Fusion Reactions as a Probe of the Nucleus-Nucleus Potential at Short Distances

Giovanni POLLAROLO

Dipartimento di Fisica Teorica, Università di Torino and Istituto Nazionale di Fisica Nucleare, Sezione di Torino, Via Pietro Giuria 1, I-10125 Torino, Italy

The semi-classical model GRAZING is used to analyze fusion excitation functions and barrier distributions for several projectile and target combinations. It is shown that the main contribution to the fusion enhancements is coming from the excitation of collective surface modes. The behavior of the fusion excitation function at very low energies is shown to be sensitive to the actual shape of the ion-ion potential at distances shorter than the position of the Coulomb barrier.

§1. Introduction

This contribution starts with an outline of the semi-classical model that is used to calculate the probability for two ions to overcome the Coulomb barrier to form a composite system at a given bombarding energy. If, afterwards, this system will equilibrate to form a compound nucleus is a question that this model, and all the others, can not answer. The calculated fusion cross sections will thus overestimate, at the higher energies, the experimental data deduced from the measurement of evaporation residue only.

Following the very brief theoretical introduction the contribution will proceed to discuss applications in actual cases stressing the role played by the different degrees of freedom in the tunneling process. Finally the behavior of the fusion excitation function at very low bombarding energies will be discussed.

§2. The semi-classical model GRAZING

Few years ago the semi-classical model for heavy ion reactions GRAZING[1)–3)] has been developed for the study of grazing reactions and the transition from the quasi-elastic to the deep inelastic regime. This model describes the evolution of the reaction by expanding the total wave function of the system $\Psi(t)$ in intrinsic states of the different asymptotic mass partitions. It incorporates, on the same footing, the excitation of the surface modes and the transfer degrees of freedom responsible for the rearrangement of mass and charge among the reactants.

The time evolution of the reaction is described by the following system of semi-classical coupled equations:

$$i\hbar\dot{c}_\beta(t) = \sum_\alpha c_\alpha(t) < \beta|H_{int}|\alpha > e^{\frac{i}{\hbar}(E_\beta - E_\alpha)t + i(\delta_\beta - \delta_\alpha)} \qquad (2\cdot1)$$

obtained from the time dependent Schrödinger equation

$$i\hbar\dot{\Psi}(t) = (H_0 + H_{int})\Psi(t) \tag{2·2}$$

by expanding, in term of channel wave functions $\psi_\alpha = \psi^a(t)\psi^A(t)e^{i\delta(\vec{R})}$, the total wave function of the system

$$\Psi(t) = \sum_\beta c_\beta(t)\psi_\beta e^{\frac{i}{\hbar}E_\beta t} \quad . \tag{2·3}$$

The time dependent coefficient $c_\beta(t)$ represents the amplitude for the system to be, at time t, in channel β. The semi-classical phase $\delta(\vec{R})$, appearing in the definition of the channel wave functions, is introduced to account for the non linear motion of the two ions in the nuclear plus Coulomb field.

With H_0 we indicated the intrinsic Hamiltonian, that for the mass partition $\alpha = (a, A)$ is written as

$$\hat{H}_0 = \sum_i^{(a)} \epsilon_i a_i^\dagger a_i + \sum_{\lambda\mu}^{(a)} \hbar\omega_\lambda \alpha_{\lambda\mu}^\dagger \alpha_{\lambda\mu} + (A) \tag{2·4}$$

and with H_{int} we represented the residual interaction responsible for the excitation of the surface modes and the exchange of nucleons,

$$\hat{H}_{int}(t) = \hat{V}_{tr}(t) + \hat{V}_{in}(t) + \Delta U_{aA}(t). \tag{2·5}$$

The residual interaction is composed of three parts; V_{in} contains the well known form-factors for inelastic excitation, V_{tr} contains the one-nucleon transfer form-factors and ΔU_{aA} the correction to the diagonal part of the interaction. The time dependence of the matrix elements is obtained by solving the Newtonian equations for the relative motion in the nuclear plus Coulomb field. For the nuclear potential we use the Akyüz-Winther[4] parametrisation that describes quite well elastic scattering data for several projectile and target combinations.

At a given bombarding energy the fusion/reaction cross section, in term of the partial wave expansion, is written,

$$\sigma(E) = \sum_\ell \frac{\pi\hbar^2}{2m_{aA}E}(2\ell + 1)T_\ell(E), \tag{2·6}$$

where $T_\ell(E)$ is the transmission probability through the potential barrier of partial wave ℓ. This, in the inverse parabolic approximation, becomes

$$T_\ell(E) = \left[1 + e^{2\pi\frac{(E_b - E)}{\hbar\omega_b}}\right]^{-1}, \tag{2·7}$$

where E_b is the barrier of the effective potential at r_b and ω_b the frequency given by

$$\omega_b = \sqrt{\frac{1}{m_{aA}}\left[\frac{\partial^2 U_{eff}}{\partial r^2}\right]_{r_b}} \quad . \tag{2·8}$$

In the calculation of $T_\ell(E)$ special attention has to be put in the definition of the capture distance, since simple classical calculations[5),6)] demonstrate that due to the excitation of the surface modes capture may arise for trajectories with an ℓ-value greater than the ℓ-grazing. In order to give an estimation of the capture angular momentum ℓ_c we look at the evolution of the distance $s(r, \alpha_{\lambda\mu})$ between the surfaces of the two nuclei. A simple inspection at the acceleration $\ddot{s}$ tells us that when this is negative very large deformations will develop; it is thus natural to search, in the multidimensional $(\vec{r}, \alpha_{\lambda\mu})$ space, the point where $\ddot{s} = 0$ and choose this point as the capture distance and the capture angular momentum ℓ_c (for more details confer Refs. 1),3)).

In the presence of couplings, the energy of relative motion is not well defined. An exchange of energy from the relative motion to the intrinsic degrees of freedom takes place, and the above formulae for the fusion cross section have to be modified to incorporate this effect. By solving in an approximate way the above system of coupled equations,[1),3)] the model calculates, for each time t, the distribution of relative motion energy E_r

$$E_r = \hat{H}(t) - \frac{(\boldsymbol{L} - \boldsymbol{I})^2 - \boldsymbol{L}^2}{2m_{aA}r^2} \quad , \tag{2·9}$$

where, with $\boldsymbol{L}$ and $\boldsymbol{I}$, we indicated the initial angular momentum and the one dissipated in intrinsic motion. The distribution in relative motion energy can be easily interpreted as a distribution of barrier height so that the actual transmission coefficient may be given by the following folding integral:

$$T_\ell(E) = \int_{-\infty}^{+\infty} P(E_r) T_\ell(E - E_r) dE_r, \tag{2·10}$$

where with $P(E_r)$ we indicated the barrier distribution. Since the barrier distribution $P(E_r)$ comes from the excitation of surface modes and transfer of nucleons, it has to be energy dependent in particular at higher energy when the transfer of angular momentum is important. It is in fact easy to show that the transfer of angular momentum modify the energy of the mode in accordance to the relation:

$$\omega \longrightarrow (\omega - \mu\dot{\Phi}(t)) \tag{2·11}$$

being $\dot{\Phi}(t)$ the angular velocity.

§3. Applications

The aim of the outlined semi-classical model is to give a unified description of elastic scattering, quasi-elastic and fusion reactions. It is thus natural to start the applications with the study of the collisions of ^{40}Ca on ^{90,96}Zr isotopes.[7)] These, in fact, are among the few reactions where, together with the fusion excitation function, quasi-elastic scattering, angular distributions and energy spectra for several transfer channels have been measured.

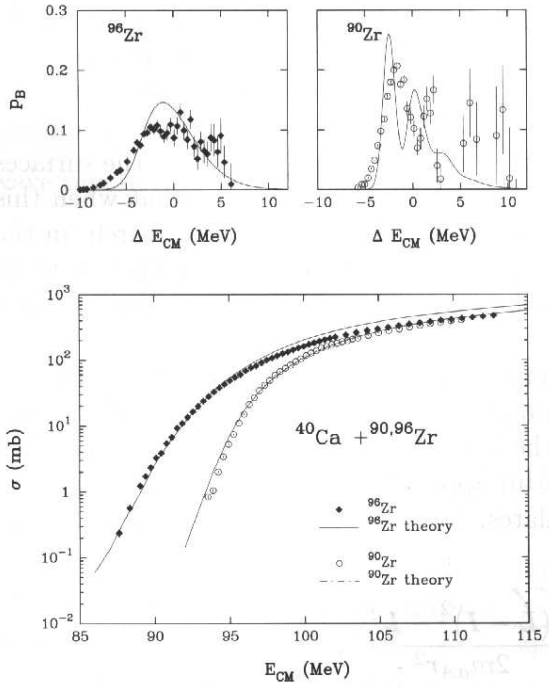

Fig. 1. Fusion excitation functions (lower panel) and barrier distributions (upper panels) for ^{40}Ca + ^{90,96}Zr, as reported in;[7] the lines are the results of GRAZING calculations.

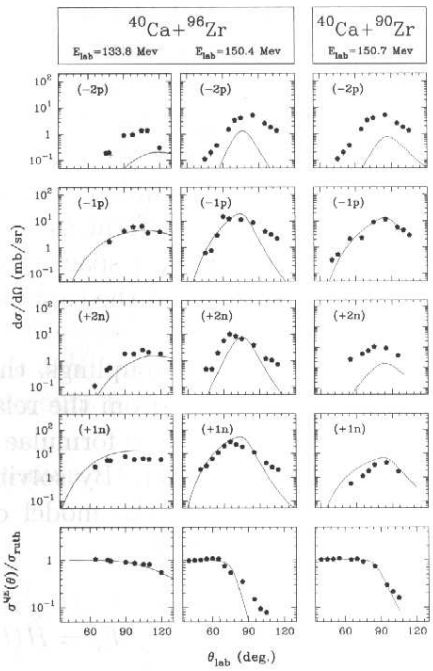

Fig. 2. Angular distributions for one- and two-particle transfer in ^{40}Ca + ^{90,96}Zr at the indicated energies. Dots are experimental values, lines are the results of GRAZING calculations.

By including the low lying 2^+ and 3^- states of projectile and target[8] and all the transfer channels (we recall that these are treated in the independent particle picture), one obtains for the fusion excitation function and barrier distributions the results shown in Fig. 1. The comparison between the experimental and theoretical barrier distributions is only qualitative since the experimental ones have been extracted from the measured excitation functions via a second order energy derivative of $E\sigma(E)$. The barrier distributions extracted with this procedure coincide with the one of the theory only if they are energy independent. In this model this is not the case. At energies larger than the Coulomb barrier, the transfer of angular momentum is important and the barrier distributions acquire all a broad Gaussian-like shape.

In Fig. 2 are shown, for the indicated bombarding energies, the angular distributions for one and two nucleon transfer channels. While the model gives a reasonable description for the neutron transfer channels and the one-proton stripping under predict the -2p channel. In the bottom row of the same figure are also reported the calculated quasi-elastic angular distributions (ratio to Rutherford) that are, in all cases, well described. This indicates that the potentials used in the calculations are reasonable. In the model there is no imaginary potential, the de-population of the entrance channel is due to the coupling to reaction channels.

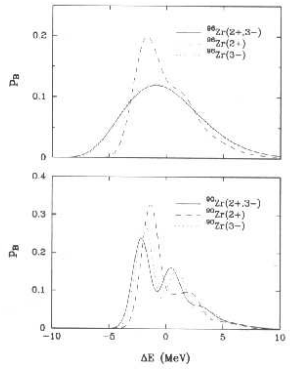

Fig. 3. GRAZING calculations for the barrier distributions in the ^{40}Ca + ^{90,96}Zr, where the contributions of various inelastic channels are evidenced.

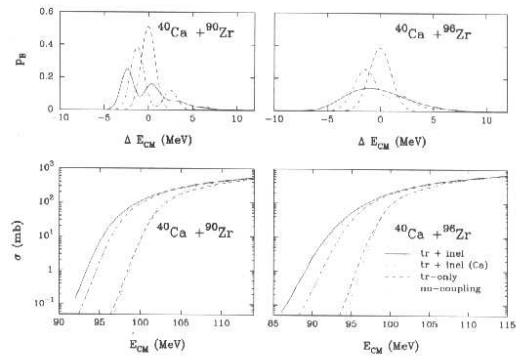

Fig. 4. GRAZING calculations of fusion for ^{40}Ca + ^{90,96}Zr, where the contributions of various channels are evidenced.

To understand why the two zirconium isotopes have a so different barrier distribution we made a detailed analysis of the contributions from the various inelastic channels. Figure 3 leads to the conclusion that the peak-less shape observed for the barrier distribution of ^{40}Ca + ^{96}Zr is essentially due to the strength of the octupole vibration in ^{96}Zr, which is more collective and lies lower in energy than in ^{90}Zr.

The various reaction channels influence differently the barrier penetrability thus, in trying to solve the old controversy among transfer and/or vibrational states, we calculated the contributions of the various couplings to the enhancements of the fusion cross sections. The results are shown in Fig. 4. It is clear that for both systems the largest contribution to the fusion enhancement is coming from inelastic excitation of the low lying states in projectile and target (being the ^{40}Ca that gives the largest contribution), the transfer channels seem to play a minor role. The importance of the high-lying modes it has also been checked, in all cases their effect may be accounted for by a small re-normalization of the strength of the real potential.

Very recently the fusion excitation function among of the same zirconium isotopes with ^{48}Ca have been measured.[9] The comparison between theory and experimental data is shown in Fig. 5. As in the previous examples, the calculations have been performed including the low lying 2^+ and 3^- states of projectile and target[8] and all the transfer channels. What makes these cases of particular interest are the barrier distributions, shown in the top frames of the figure. The two curves represent barrier distributions at two different bombarding energies (they differ by ~15 MeV). The ^{96}Zr reaction displays a barrier distribution that is almost energy independent. This is the ideal case to check if the barrier distribution obtained from the second order energy derivative of the $E\sigma(E)$ is connected to the "true" barrier distribution that reflects the coupling to the degrees of freedom of target and projectile. In Fig. 6 we display the comparison between the theoretical barrier distribution (dotted line) and the ones extracted from the calculated excitation function. This last procedure indeed reproduces quite well the excitation function if, in taking the derivative, one uses a small energy step (0.2 MeV in this case). If one uses a larger energy step, very close to the one of the experiment, the obtained barrier distribution is quite

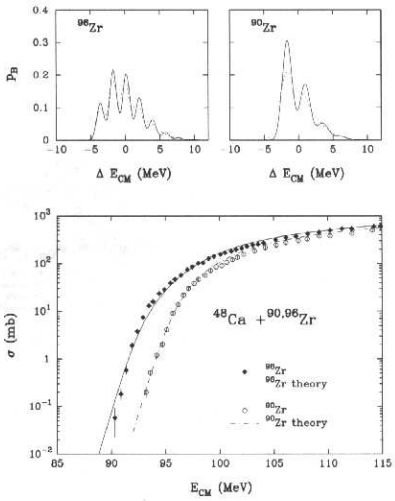

Fig. 5. GRAZING calculations of fusion excitation function for ^{48}Ca + ^{90,96}Zr in comparison with thre experimental data.[9] In the top are shown the calculated barrier distribution for two bombarding energies (see text).

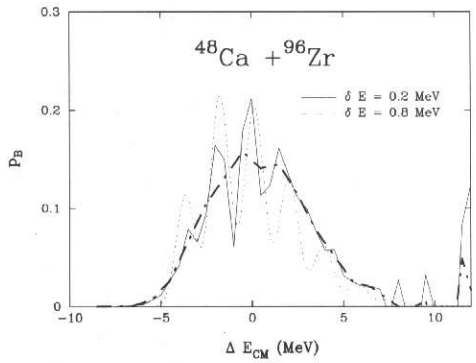

Fig. 6. Comparison between the theoretical barrier distribution (dotted line) and the one extracted from the fusion excitation function via second order energy derivative of $E\sigma(E)$. The full line corresponds to an energy step of 0.2 MeV, while the dash-dotted line corresponds to an energy step of 0.8 MeV (similar to the one of the experimental data).

different, it looses all the structure. This is clearly a warning to the actual content of the barrier distributions extracted from the experimental excitation functions. A little more caution should be used in the comparison with the theoretical one.

§4. Fusion at very low energies

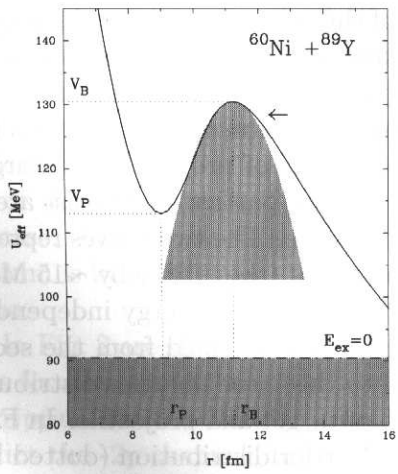

Fig. 7. The nucleus-nucleus potential for a head-on collision ($\ell = 0$) in the reaction ^{60}Ni + ^{89}Y. Shown in the figure is also the parabolic approximation.

Measurements of sub-barrier fusion cross sections may become an effective tool[10] to shed light on the characteristics of the nuclear potential at distances shorter than the Coulomb barrier. In fact, the standard approach to investigate these reactions exploits the mechanism of barrier penetration in the presence of couplings to intrinsic degrees of freedom.[11)–15)] Crucial to the success of these analyses is a proper adjustment of the height and thickness of the potential barrier for small partial waves ($\ell \approx 0$). While the former controls displacements in the energy scale, the barrier width is related to the exponential slope $2\pi/\hbar\omega_b$ of the function $\sigma(E)$ at the lowest energies.

The drastic exponential drop associated with the characteristic values of $\hbar\omega_b$ has limited in practice the range of measured cross section to only a few MeV below the Coulomb barrier. In such case the parabolic approximation remains valid. A pioneering experiment done in Argonne[16] has gone to very low energies showing that here the fusion cross section drops faster than the expected exponential behavior.

A large number of ion-ion potentials predict a pocket in the inner region, as is illustrated in Fig. 7. Here we see the profile of a frequently used ion-ion potential (the Akyüz-Winther potential of Ref. 4)). Shown in the figure is also the absolute limit to fusion that comes from the required exothermic character of the process. This energy is far below the relative one quenching the tunneling process, V_P, and therefore it is clear that the latter takes precedence as a limiting mechanism causing,

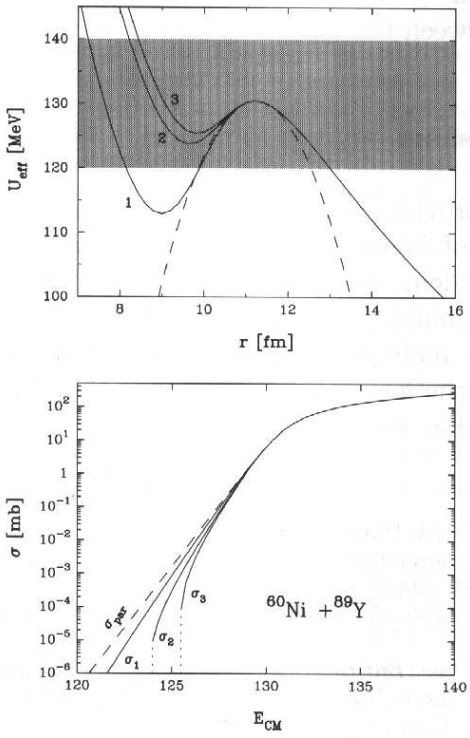

Fig. 8. Top, three possible ion-ion potentials which have an identical radial dependence for $r > 11.01$ fm. Bottom, the fusion excitation function for the potentials shown above. $\sigma_{par}(E)$ is the cross section within the parabolic approximation.

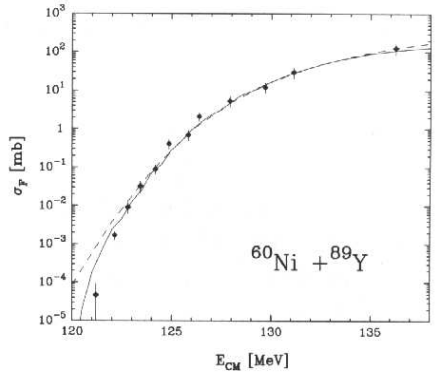

Fig. 9. Fusion excitation function as calculated from GRAZING for the indicated system in comparison with the experimental data. Also shown (dash-line) are the results using the analytical expression for the transmission coefficient.

$\log\sigma(E) \to -\infty$. Deviations from the parabolic approximation should be expected to show up even much earlier as the bombarding energy is gradually reduced below the barrier. A simple, visual estimation of the value of energy where this would happen is shown by the arrow, less than 5 MeV below the barrier.

To show that it is possible to learn about the shape of the potential in the inner side of the potential barrier we start by studying the fusion cross sections in the absence of interactions. How the couplings to different reaction channels affect the so-called "reference" curve has been extensively covered in the literature[11)–15)] and we know that the final results at the lowest bombarding energies always inherit (or build upon) whatever characteristics are already present in the simplest barrier-penetration formulation of the problem. At low energy, lower than the one indicated

with an arrow in Fig. 7, we cannot rely in the analytic form of the transmission coefficients for a parabolic barrier and we shall use, in what follows, their WKB expression.[4] Taking a family of hypothetical potentials, shown at the top of Fig. 8, that are identical for large values of r and which share the same values of V_B, r_B and $\hbar\omega_B$ we obtain for the fusion excitation function the results show at the bottom of the same figure. It is clear that the drop of the fusion cross sections follows the different values of the inside pocket of the potentials.

To demonstrate that the above picture is not destroyed by the coupling, GRAZING has been modified to accept the new potentials and to use the WKB expression for the transmission coefficient. The results of such calculations are shown in Fig. 9 for the potential labelled 3 in Fig. 8. The shallow pocket of the potential will not only influence the fusion cross section at low energies but it will modify the sharing, of the total reaction cross section reaction between fusion and deep-inelastic clearly in favor of the last.

§5. Conclusions

The semi-classical model presented here provides a very effective tool to understand the role played by the intrinsic degrees of freedom in the enhancement of the fusion cross section. The main effect has been demonstrated to come from the excitation of the surface modes and the transfer channels play only a minor role (at high energy they are very important providing the main mechanism for the dissipation of energy). It has also been shown that from the low energy behavior of the fusion cross section one can learn about the potential at very short distances.

References

1) A. Winther, Nucl. Phys. A **572** (1994), 191; Nucl. Phys. A **594** (1995), 203.
2) A. Winther, GRAZING, Computer Program, unpublished.
3) G. Pollarolo and A. Winther, Phys. Rev. C **62** (2000), 054611.
4) R. Broglia and A. Winther, *Heavy Ion Reactions* (Addison-Wesley Pub. Co., Redwood City CA, 1991).
5) R. A. Broglia, C. H. Dasso and A. Winther, *Proc. Enrico Fermi Intern. School of Physics 1979*, eds. R. A. Broglia, C. H. Dasso and R. Ricci (North-Holland, Amsterdam, 1981).
6) C. H. Dasso and G. Pollarolo, Comput. Phys. Commun. **50** (1988), 341.
7) G. Montagnoli et al., Eur. Phys. J. A **15** (2002), 351.
8) M. R. Bhat, Nucl. Data Sheets **82** (1997), 547.
9) F. Scalassara, Prog. Theor. Phys. Suppl. No. 154 (2004), 31.
10) G. Pollarolo and C. H. Dasso, to appear in Phys. Rev. C.
11) H. Esbensen, Nucl. Phys. A **352** (1981), 147.
12) C. H. Dasso, S. Landowne and A. Winther, Nucl. Phys. A **405** (1983), 381.
13) C. H. Dasso and S. Landowne, Comput. Phys. Commun. **46** (1987), 187.
14) H. Esbensen and S. Landowne, Phys. Rev. C **35** (1987), 2090.
15) K. Hagino, N. Rowley and A. T. Kruppa, Comput. Phys. Commun. **123** (1999), 143.
16) C. L. Jiang et al., Phys. Rev. Lett. **89** (2002), 052701.